Investigating Interactions Mediated by the Presynaptic Protein Bassoon in Living Cells by Foerster's Resonance Energy Transfer and Fluorescence Lifetime Imaging Microscopy

Mini Jose,* Deepak K. Nair,* Wilko D. Altrock,* Thomas Dresbach,† Eckart D. Gundelfinger,* and Werner Zuschratter*

*Leibniz Institute for Neurobiology, Magdeburg, Germany; and †Institute for Anatomy and Cell Biology, University of Heidelberg, Heidelberg, Germany

ABSTRACT Neuronal synapses are highly specialized structures for communication between nerve cells. Knowledge about their molecular organization and dynamics is still incomplete. The large multidomain protein Bassoon plays a major role in scaffolding and organizing the cytomatrix at the active zone of neurotransmitter release in presynaptic boutons. Utilizing immunofluorescence techniques, we show that Bassoon is essential for corecruitment of its synaptic interaction partners, C-terminal binding protein 1/brefeldin A-dependent ADP-ribosylation substrate and CAZ-associated structural protein, into protein complexes upon heterologous expression in COS-7 cells. A combination of Foerster's resonance energy transfer and fluorescence lifetime imaging microscopy in the time domain was adopted to investigate the potential for the association of these proteins in the same complexes. A direct physical association between Bassoon and CtBP1 could also be observed at synapses of living hippocampal neurons. Simultaneous analysis of fluorescence decays of the donor and the acceptor probes along with their decay-associated spectra allowed a clear discrimination of energy transfer.

INTRODUCTION

Making use of the current advances in fluorescence microscopy and the development of variants of green fluorescent proteins (GFPs), Foerster's resonance energy transfer (FRET) is becoming a powerful tool to map protein-protein interactions in living specimens. In contrast to in vitro methods, which are useful to assess the potential of proteins for physical interactions, FRET allows direct access to these interactions within a macromolecular complex inside a living cell at nanometer resolution (1,2). FRET combined with fluorescence lifetime imaging microscopy (FLIM) is gaining importance as a powerful technique in probing these interactions in biological systems at the molecular level due to its independence from excitation intensities and fluorophore concentrations (3,4). The advantage of using the contributions of lifetimes or decay-associated spectra (DAS) by simultaneous donor-acceptor analysis to discriminate FRET in biological samples has been shown in previous works (5,6). Thus, a combination of these techniques provides high spatial (nanometer) and temporal (picosecond) resolution in monitoring interactions within protein complexes in their natural environment.

Active zones are specialized regions of the presynaptic plasma membrane designed for the regulated exocytosis of neurotransmitters. A highly organized cytomatrix of proteins assembled at the active zone, i.e., the cytomatrix at the active zone (CAZ), is thought to mediate and regulate membrane trafficking events underlying neurotransmitter release (7,8). Bassoon and its sister molecule Piccolo are major scaffolding components of the CAZ (9,10). The CAZ-associated structural protein CAST/ELKS2 (11–13) and the C-terminal binding protein 1/brefeldin A (BFA)-dependent ADP-ribosylation substrate (CtBP1/BARS) (14) have been suggested to directly interact with Bassoon-containing complexes, though the clear functional relevance of these interactions is yet to be addressed. CtBP1/BARS plays a key role as a transcription corepressor during embryonic development and in oncogenesis, and as a promoter of Golgi membrane fission in intracellular trafficking (15).

It has been shown biochemically that a central fragment of Bassoon of ~1500 amino acids (Bsn1692-3263) (16) has the potential to interact with CtBP1 (14), while it also harbors the binding site for CAST/ELKS2 (11). Upon blockade of the Golgi exit in neurons or upon expressing heterologously in nonneuronal cells, Bassoon forms protein clusters in the cell soma (17). It would be interesting to know whether these macromolecular complexes are functional and can recruit binding partners of Bassoon. A deeper understanding of the nature of the association of CAZ proteins with these complexes is also crucial in providing insight into their basic molecular network. In neurons, though Bassoon and CtBP1 are colocalized in synapses (14), a direct physical interaction between them at these sites in living cells has not yet been proven. A direct confirmation of such an in vivo interaction would provide deeper insight into the molecular organization of the CAZ.

Neuronal development is characterized by high ionic changes that significantly affect the properties of fluorescent

Submitted April 27, 2007, and accepted for publication September 26, 2007.

Mini Jose and Deepak K. Nair contributed equally to this work.

Address reprint requests to Mini Jose, Leibniz Institute for Neurobiology, Brenneckestrasse 6, 39118 Magdeburg, Germany. Tel.: 49-391-626-3704; Fax: 49-391-626-3328; E-mail: mini.jose@ifn-magdeburg.de.

Editor: David W. Piston.

0006-3495/08/02/1483/14 $2.00

doi: 10.1529/biophysj.107.111674

probes (6,18). Therefore, in this study, heterologous expression in COS-7 cells was initially used to assess the formation of macromolecular complexes involving CtBP1 and CAST recruited by Bassoon. This system also provided an environment free of Piccolo, the sister molecule of Bassoon, another potential binding partner of both CtBP1 (14) and CAST (11). Here, we assessed the role of Bassoon in organizing macromolecular complexes linking its different synaptic interaction partners. Bassoon-dependent recruitment of CtBP1 was studied using different functional fragments of Bassoon, including the short central fragment (Bsn1692-3263). A combination of FRET and time domain FLIM was utilized for monitoring a direct physical association of these proteins in living COS-7 cells. Similar approaches were adopted for a deeper understanding of the association of Bassoon and CtBP1 in presynaptic complexes of living hippocampal neurons. A combination of recently generated photostable variants of cyan fluorescent protein (CFP) and yellow fluorescent protein (YFP), namely Cerulean and Citrine (19,20), was used as a suitable donor-acceptor pair for the purpose. Unlike the conventional way of monitoring donor mean lifetimes alone, simultaneous multi-exponential analysis of donor and acceptor fluorescence decays along with DAS allowed the discrimination of excited state reactions, such as energy transfer.

MATERIALS AND METHODS

Cloning

The central fragment of Bassoon complementary DNA (cDNA) encoding amino acid residues 1692-3263 (Bsn1692-3263, see Fig. 7) (16) was cloned into a frame-shifted variant of p-Cerulean or pCMV-Tag2A expression vectors using *Bam*HI/*Bam*HI restriction sites, and CtBP1 cDNA (14) was cloned into frame-shifted variants of p-Cerulean (19) and p-Citrine (20) using *Eco*RI/*Xho*I restriction sites introduced via linkers. Full-length Bsn cDNA (16) was subcloned from a cloning vector into p-Cerulean or pCMV-Tag2A using *Not*I sites. Bsn1692-3263 and full-length Bsn lacking the fluorescent tag are referred to as the untagged Bsn1692-3263 and untagged full-length Bsn, respectively. CAST/ELKS2 (11,13) was cloned into p-Cerulean and p-Citrine expression vectors using *Bam*HI/*Sac*I restriction sites. The frame-shifted variants of p-Cerulean and p-Citrine were generated using standard molecular biological techniques. Bsn or *bsn* is the official abbreviation in databases for the Bassoon protein and gene, respectively. In this article, we have used the abbreviation to name all cDNA constructs. The numbers indicate the amino acids covered by the cDNA.

Cell cultures, transfection, and immunocytochemistry

COS-7 cells were grown in DMEM (Dulbecco's modified Eagle's medium, Invitrogen, Karlsruhe, Germany) that included 10% fetal calf serum (FCS), antibiotics (100 units/ml penicillin, 100 μg/ml streptomycin), and 2 mM glutamine at a density of 10^5 cells per well (0.5 ml) at 37°C, 5% CO_2 environment. Hippocampal neurons from rat brains of embryonic day 19 were cultured in DMEM that included 10% FCS, antibiotics (100 units/ml penicillin, 100 μg/ml streptomycin) and 2 mM glutamine. The neurons were grown at a density of 60,000 cells/0.5 ml in Neurobasal medium (without phenol red, Invitrogen) containing B27, antibiotics (100 units/ml penicillin, 100 μg/ml streptomycin), and 2 mM glutamine. COS-7 cells and neurons were transfected with Cerulean, Citrine, or fusion constructs of full-length Bsn, Bsn95-3938, Bsn1692-3263 (16), CtBP1, or CAST cDNAs using Polyfect Transfection Reagent (Qiagen, Hilden, Germany) and Lipofectamine (Invitrogen), respectively. The cells were fixed with 4% paraformaldehyde (PFA) in phosphate buffer saline and immunostained with primary antibodies against CtBP1 (mouse, 1:1000, BD Transduction Laboratories, Lexington, CA), Bassoon (mouse/rabbit, 1:1000) (9), CAST (rabbit, 1:200, Synaptic Systems, Goettingen, Germany), or SAP90/PSD-95 (rabbit, 1:200, Synaptic Systems). Alexa 594 (anti-mouse/-rabbit, 1:200, Molecular Probes, Eugene, OR), Alexa 488 (anti-rabbit, 1:200, Molecular Probes), and Cy3 (anti-mouse, 1:100, Dianova, Hamburg, Germany) were used as secondary antibodies. Primary antibody incubation was done overnight at 4°C.

Quantification

Fluorescence quantification experiments were performed using Leica-TCS-SP2-AOBS (63× oil immersion objective, Leica Microsystems, Mannheim, Germany). To quantify the nuclear expression of CtBP1 (Supplementary Materials Fig. 1), COS 7 cells were transfected with Cerulean-Bsn1692-3263, fixed, and immunostained with anti-CtBP1 (mouse, 1:1000) with the protocols mentioned previously. Alexa 594 (anti-mouse, 1:200) was used as the secondary antibody. Confocal stacks of 18 sections with a section size of 0.60 μm were collected. The maximum projection images of the stacks were taken, and the fluorescence quantified using Image J 1.38. The expressions of CtBP1 in transfected and untransfected cells of the same stacks were compared. To quantify the Bassoon fluorescence at synaptic sites (Supplementary Material Fig. 2), mature neurons (after 15 days in vitro (DIV 15)) were transfected with Cerulean full-length Bsn. The cells were fixed 14–15 h after transfection and immunostained with anti-Bassoon (mouse, 1:1000, Stressgen, North Yorkshire, UK) and anti-SAP90/PSD-95 (rabbit, 1:200); the latter served as a postsynaptic marker. Cy3 (anti-mouse, 1:100) and Alexa 594 (anti-rabbit, 1:200) were used as secondary antibodies. Untransfected cultures subjected to the same treatment, which were measured under similar excitation and detection conditions, were used as control. Confocal stacks of 24 sections with a section size of 0.28 μm were collected. Image processing and fluorescence quantification were performed as for COS-7 cells.

For quantitative Western blot analysis (Supplementary Material Fig. 3), Citrine-CtBP1 transfected COS-7 cells were harvested in lysis buffer (150 mM NaCl, 1% TritonX-100, complete protease inhibitor (Roche Applied Science, Mannheim, Germany), 10 mM TrisHCl pH 7.4). Proteins were precipitated, each sample was loaded as a triplet on a Tris-acetate buffered gel, and after separation proteins were transferred to an Immobilon fluoropolymer polyvinylidene difluoride membrane (Millipore, Schwalbach, Germany) as previously described (14). Blots were incubated with anti-CtBP1 (mouse, 1:5000) as primary and anti-mouse immunoglobulin G-Alexa 680 (Invitrogen) as secondary antibodies and scanned on an Odyssey Imager (LI-COR, Bad Homburg, Germany) according to the manufacturer's protocols. Fluorescence intensities of bands for endogenous CtBP1 and Citrine-CtBP1 were determined with Odyssey Application Software 2.1 (LI-COR).

Steady-state imaging

The cells were imaged in an extracellular buffer (pH 7.4, 129 mM NaCl, 5 mM KCl, 2 mM $CaCl_2$ $2H_2O$, 1 mM $MgCl_2$ $6H_2O$, 20 mM Hepes, 30 mM Glucose). To perform steady-state imaging, the microscope was equipped with a charge-coupled device (CCD) camera (F View, SIS Imaging Systems, Duesseldorf, Germany). The filter settings (AHF Analysentechnik, Tuebingen, Germany) used were D436/20 excitation filter, 455 DCLP dichroic beam splitter, and D480/40 emission filter for Cerulean and HQ 500/20 excitation filter, Q515 LP dichroic beam splitter, and HQ 535/30 emission filter for Citrine. Only the cells showing moderate expression levels of transfected constructs were used for imaging. Confocal fluorescence images as well as differential interference contrast (DIC) images were captured using Leica-TCS-SP2-AOBS (Leica Microsystems).

FLIM system

A femtosecond mode-locked titanium sapphire laser (Tsunami Model 3955, 690–1080 nm, 80 MHz, Spectra Physics, Mountain View, CA) pumped by a continuous diode laser (Millennia Vs, 5W, TEM_{00} 532 nm, Spectra Physics) was tuned and frequency doubled using a frequency doubler/pulse picker (Model 3986, Spectra Physics) to the desired wavelength of 420 nm with a pulse repetition rate of 8 MHz. The excitation probability at this wavelength was >80% for Cerulean, whereas for Citrine it was <5% (21). The laser beam was coupled alternatively via two optical fibers to different ports of an inverted microscope (IX81, Olympus, Hamburg, Germany). The beam was directed to the sample after passing a beam splitter, 450 DCLP (AHF Analysentechnik), and an oil immersion 100× objective (Plan Apo 100×/1.45 oil, total internal reflection fluorescence microscopy, Olympus). The system allowed illumination of the sample for the two types of detectors. The delay line (DL) and quadrant anode (QA) detectors (Europhoton, Berlin, Germany) (22), based on time- and space-correlated single photon counting, were used to study the interaction between tagged fluorophores by simultaneous acquisition of time and space information on a picosecond timescale. More detailed discussions of the FLIM system are presented in Jose et al. (6) and Nair et al. (5).

A focused beam in combination with an iris was used to limit the area of excitation for recording using the DL detector. The fluorescence emissions from the tiny selected area passed an emission filter, HQ 460 ALP (AHF Analysentechnik), and the slit (11 mm × 0.10 mm) of the polychromater fixed in front of the sensitive area of the point detector to translate the spectrally resolved intensity decays on the detector. Whole field illumination was provided for the QA detector, which imaged the fluorescence decays simultaneously within the whole illuminated region. The fluorescence emission was split by a beam splitter (dichroic 505 DCXR) and passed into two specific wavelength bands defined by the band-pass emission filters, D 480/40 M for Cerulean and 540/40 ALP for Citrine. This allowed the simultaneous monitoring of donor and acceptor dynamics.

The pulse width of the instrument response function (IRF) in the point detector (DL) was reduced to a minimum of 150 ± 25 ps, measured at full width half-maximum. The wavelength sensitivity of the system was calculated to be 1.02 nm/channel. The time channel resolution of the point detector was calculated to be 24.81 ps/channel. The pulse width of the IRF of the imaging detector (QA) was reduced to a minimum of 200 ± 20 ps at full width half-maximum. The time channel resolution of the imaging detector was calculated to be 9.72 ps/channel. Independent control measurements of the monoexponential dye coumarin6 in ethylene glycol at magic angle, excited at 420 nm, and observed in a band of 515 ± 15 nm (HQ 515/30, AHF Analysentechnik) were performed to ensure the absence of any systemic effects. Lifetimes of 2.30 ns and 2.29 ns were obtained for the point and imaging detectors, respectively; these were similar to the published value of 2.30 ns (23).

Data analysis

The data analysis has been discussed in previous works (5,6). To obtain lifetimes from fluorescence decays, the data were modeled by the convolution product of a multiexponential theoretical model with the IRF: $i(t) = \mathrm{IRF}(t) \otimes \Sigma \alpha_i e^{-t/\tau i}$, where α_i is the relative contribution of the fluorescent species characterized by the fluorescence lifetime, τ_i, and IRF is the measurement of the pulsed excitation. Data were analyzed by the Levenberg-Marquardt nonlinear least-squares algorithm using the Globals Unlimited software package (version 1.20) (24). The quality criterion for global fit was defined as $\chi^2 < 1.3$ for all analyzed decays. The criteria for the improvement of χ^2 upon addition of multiexponential components were set to a value of $\Delta\chi^2$—the ratio between the χ^2 of the previous model and the current model with the addition of a single lifetime component, where $\Delta\chi^2 > 1.05$. χ^2 was checked using the linked multiexponential model and the unlinked model, and the data set was discarded if the ratio of χ^2 was >1.05, indicating a random error originating from the data acquisition.

Rigorous error analysis using global analysis software was performed to obtain a realistic estimation of the variation of χ^2 associated with each lifetime. A set of intervals was defined for each analyzed lifetime in the model. The values of the upper and lower limits for the interval were set to a 20% variation for the long lifetimes (τ_1 and τ_2) in all cases. The variation was increased to 60% for τ_3 to obtain a realistic spread of the χ^2 minimum surface. The number of points between the upper and lower limits was set to 10. The examined parameter was fixed at the current trial value, but all other parameters were allowed to vary to minimize the value of χ^2. A plot of the change of χ^2 with the change in lifetimes was obtained (Supplementary Material Fig. 4 *c*). The maximum error on the lifetimes corresponding to 67% χ^2 confidence was deduced from this plot. Comparison of these results with the obtained multiexponential model was used to judge the quality of lifetimes in the fit. At 67% χ^2 confidence, the maximum error for the individual lifetimes obtained was in the range 0.07–0.11 ns for all samples.

Data obtained from the point detector were fit with linked lifetimes for the decays corresponding to the different emission wavelength bands. The individual decays were obtained by binning data over a fixed number of continuous wavelength channels, resulting in a net resolution of 7.14 nm per decay. The contributions of the lifetimes in each of these intensity decays were obtained as preexponential factors α_i. α_i was plotted along the wavelength to obtain the DAS. The preexponential factor α_i, corresponding to a lifetime in an intensity decay, was positive except in the case of excited state reactions, where it changes to negative (25). The comparison of plots of DAS of different multiexponential components allowed us to discriminate among the fluorescent species involved in different excited state processes. The fractional contributions were calculated as $|\alpha_i|/\sum|\alpha_i|$ for the different exponentials in the model. The mean lifetime τ_{mean} of each intensity decay was calculated as $\tau_{mean} = \sum|\alpha_i\tau_i|/\sum|\alpha_i|$, where τ_i is the lifetime and α_i is the corresponding preexponential factor in the decay. There was no averaging over the entire spectra, since mean lifetimes as well as the contributions of multiple lifetimes were wavelength dependent. The individual counts at the peak for each analysis were maintained at 6000–7000. Data were acquired continuously for 10–15 min using the point detector to get the required photons for analysis.

Data obtained by the imaging detector were analyzed by selecting corresponding regions of interest (ROIs) for the Cerulean and Citrine channels, as defined by the filter settings. The data sets of individual channels were exported to the Globals Unlimited software format. The donor and acceptor decays were analyzed with linked lifetimes. The peak counts were always ensured to be >10,000. Continuous measurements of 15–20 min were performed using the imaging detector.

The FRET efficiency was calculated as $E = 1 - \tau_{DA}/\tau_D$, where τ_D is the unperturbed mean lifetime of the donor and τ_{DA} is the mean lifetime of the donor in the presence of an acceptor or the FRET lifetime. The lifetime maps were generated using the QA Analysis software (Europhoton), fitting from the peak of the intensity decay. An estimate of the background was performed by obtaining mean counts per pixel of areas of background and then subtracting this level from the whole field image. A lifetime map was then produced by assigning a color on a 16-bit pseudocolor scale to a fitted single-exponential decay time. The resulting pseudocolor lifetime image was displayed over 1.1–3.1 ns; this was used to analyze the morphological variation of lifetimes in cells in detail.

RESULTS

Colocalization studies of Bassoon and its interaction partners in COS-7 cells and neurons

It has been proposed that the presynaptic protein Bassoon interacts with both CtBP1 (14) and CAST (11) and that these interactions contribute to the molecular organization of the active zone of neurotransmitter release. To characterize these interactions in living cells, we used a heterologous expression of these binding partners in COS-7 cells. As Bassoon forms macromolecular complexes in the cytoplasm when

expressed in nonneuronal cells (17), we tested whether Bassoon is functional within these complexes, i.e., whether it can recruit its binding partners.

Immunofluorescence studies with antibodies against CtBP1 showed a nuclear localization (Fig. 1, *a–c*), which changed significantly in the presence of a Bassoon construct similar to the full-length, namely, Bsn95-3938 (16) (Fig. 1, *d–f*). In COS-7 cells, which endogenously do not express Bassoon, the protein showed the expected punctate pattern when expressed heterologously (Fig. 1 *d*). In this case, the nuclear staining of CtBP1 was significantly reduced with increased immunoreactivity in Bassoon-containing macromolecular complexes in the cytosol. Using a fragment of Bassoon (Bsn1692-3263, see Fig. 7), which in neurons is still recruited to the presynapse, a similar change in the distribution of CtBP1 immunoreactivity was observed (Fig. 1, *g–i*). Quantitative analysis revealed a 1.4-fold reduction of CtBP1 immunoreactivity in the nucleus of COS-7 cells in the presence of Cerulean-Bsn1692-3263 ($n = 100$, Supplementary Material Fig. 1). Thus, clear interference with the nuclear recruitment of CtBP1 was observed in the presence of both Bassoon constructs. Coexpression of Bassoon (Bsn95-3938 or Bsn1692-3263) with CAST in COS-7 cells followed by CtBP1 immunostaining revealed a corecruitment of CtBP1 and CAST to the Bassoon-containing molecular complexes (Fig. 2, *a–d*). No such extranuclear recruitment of endogenous CtBP1 was observed in the presence of CAST alone (Fig. 2, *e–g*).

When expressed in young neurons at DIV 7, a similar recruitment of CtBP1 and CAST to the Bassoon-containing complexes (Fig. 3, *a–d*) was also observed with Bsn1692-3263. In mature neurons at DIV 16, CtBP1 colocalized with Bassoon-containing complexes along axons, most likely representing presynapses (Fig. 3, *e–g*, (14)). Quantification of overexpression levels of Bassoon indicated a fivefold increase at synapses ($n = 5000$ from 10 independent experiments, Supplementary Material Fig. 2). These findings suggest that Bassoon has a role in recruiting its binding partners to protein complexes at presynaptic active zones.

Photophysics of Cerulean and Citrine in living cells

The photophysical properties of the common fluorescent probes CFP and YFP have been observed to be perturbed by cellular environments (6). Therefore, it was crucial to understand the behavior of photostable variants of them, namely Cerulean and Citrine, used for the FRET-FLIM studies in living cells.

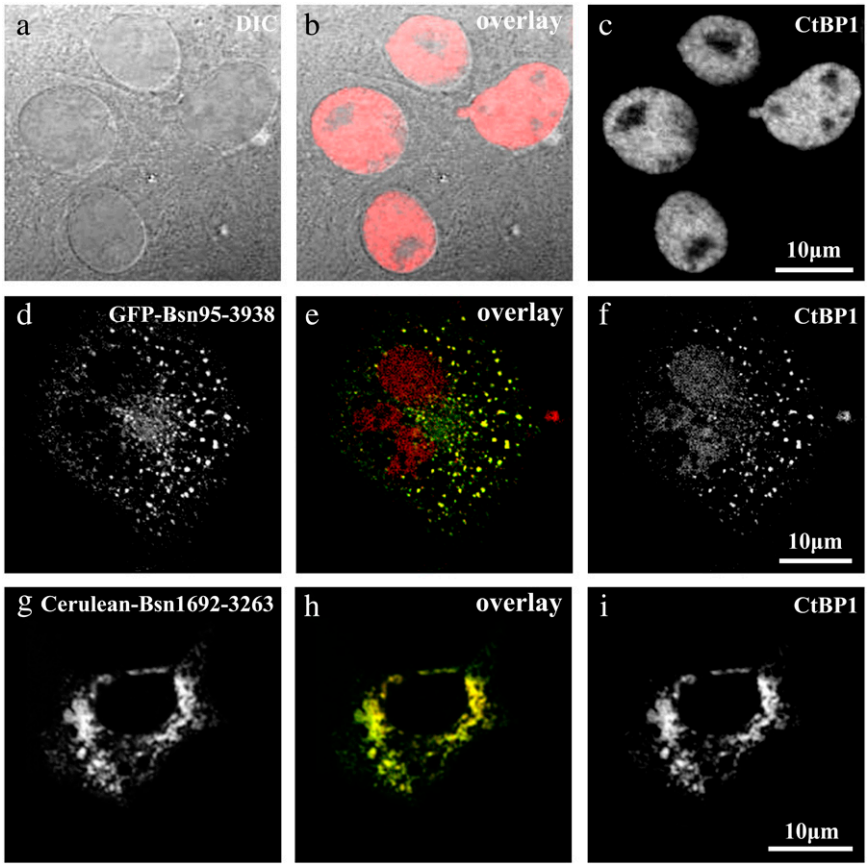

FIGURE 1 Immunofluorescence of CtBP1 in COS-7 cells in the absence and presence of Bassoon. (*a–c*) DIC images (*a*) together with immunostainings against CtBP1 (*c*) of the same cells showed clear nuclear localization of CtBP1. (*d–i*) Disruption of the nuclear localization of CtBP1 (*f* and *i*) in the presence of a Bassoon construct similar to the full length, namely, Bsn95-3938 (*d*) as well as in the presence of Bsn1692-3263 (*g*). In the overlay images (*e* and *h*), GFP-Bsn95-3938 and Cerulean-Bsn1692-3263 are shown in green, whereas endogenous CtBP1 stained with Alexa 594 is shown in red. Yellow denotes the degree of colocalization of these proteins. In both cases, CtBP1 was enriched outside the nucleus in contrast to its original localization pattern.

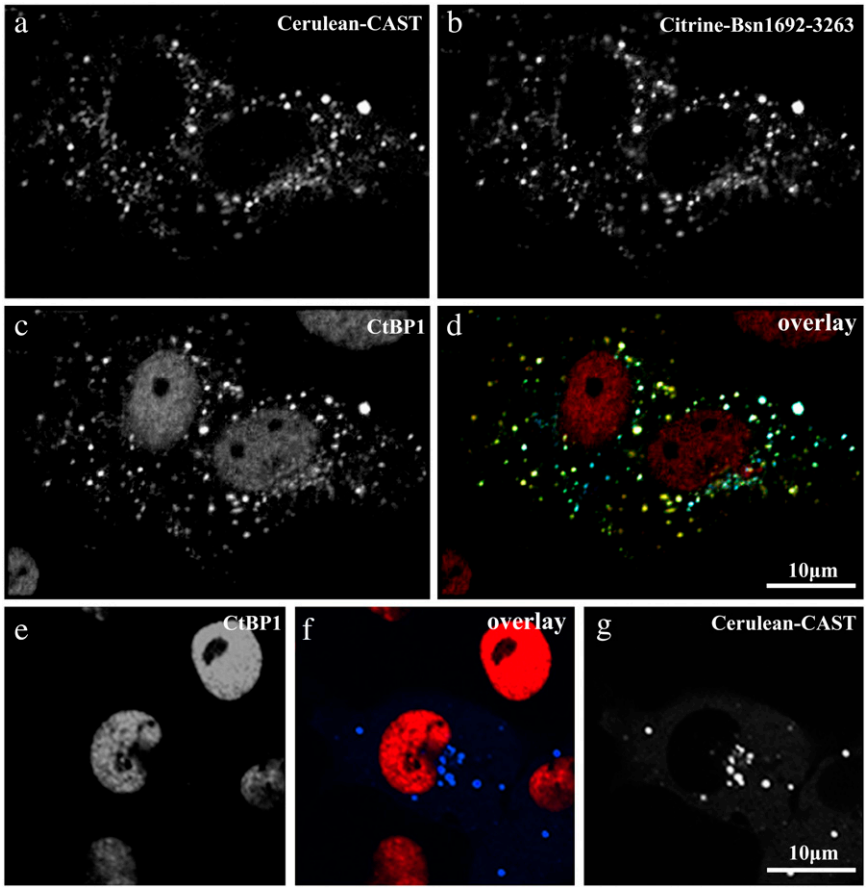

FIGURE 2 Corecruitment of Bassoon, CtBP1, and CAST to the same intracellular complexes in COS-7 cells (*a–d*). Cells were transfected with Cerulean-CAST (*a*) and Citrine-Bsn1692-3263 (*b*) and immunostained with antibodies against CtBP1 (*c*). The overlay of the trimeric complex is given in (*d*), where Cerulean-CAST, Citrine Bsn1692-3263, and CtBP1 are shown in green, red, and blue, respectively. (*e–g*) In the absence of Bassoon, the presence of CAST did not affect the nuclear localization of endogenous CtBP1. Cerulean-CAST (*g*) was observed to form cytosolic complexes, but no extranuclear recruitment of CtBP1 to these complexes was observed as visualized by Alexa 594 immunostainings (*e*).

COS-7 cells expressing Cerulean alone showed emission maxima at 486 nm (Fig. 4 *a*). In contrast to the monoexponential fluorescence decay previously reported in solutions (19), a biexponential decay was observed for Cerulean in living COS-7 cells with lifetimes of 3.37 ± 0.03 ns (τ_1) and 1.32 ± 0.05 ns (τ_2) (Table 1, Fig. 4 *b*). DAS revealed similar distributions for the lifetimes, confirming the source of both lifetimes to be the Cerulean chromophore (Fig. 4 *c*). The quality of decay fits is presented in Supplementary Material Fig. 4, *a* and *b*. The rigorous error analysis of multiple lifetimes was performed to ensure the reliability of the values (Supplementary Material Fig. 4 *c*). The mean lifetime at the donor emission maxima was calculated to be 2.46 ± 0.04 ns, which did not show any deviation along the wavelength axis (Fig. 4 *d*). The advantage of FRET determination by donor excitation and simultaneous analysis of donor and acceptor emission was signified by coexpressing Cerulean with a stable variant of YFP called Citrine. The fluorescence emission spectra or decay of this mixture were not different from those of Cerulean, except for a small emission near the YFP peak (Fig. 4, *a* and *b*) arising due to the high molar extinction coefficient of Citrine (20). Direct excitation of Citrine alone at 420 nm resulted in a single lifetime of 3.20 ± 0.03 ns contaminated by a short lifetime contribution of 0.22 ± 0.14 ns. The latter arose most likely from cell autofluorescence, as observed from the DAS (Supplementary Material Fig. 4 *d*), which showed a completely different distribution compared to the 3.20 ns component.

Interaction studies of the trimeric complex Bassoon, CtBP1, and CAST by FRET-FLIM in living COS-7 cells

To achieve deeper insight into the interactions and complex formation of the different CAZ proteins including Bassoon, CtBP1, and CAST, the colocalization studies of these proteins were extended to live cell interaction studies by FRET and FLIM. Different binding strategies with Cerulean- and Citrine-fused constructs as donor-acceptor pair were adopted for this purpose, as discussed below.

Interaction studies of Bassoon and CtBP1

Though the possibility for binding between Bassoon and CtBP1 has been indicated by biochemical techniques (14), a confirmation of this interaction under real cell conditions was crucial to appreciate its physiological relevance. Since the Cerulean full-length Bsn was too dim for FRET studies with

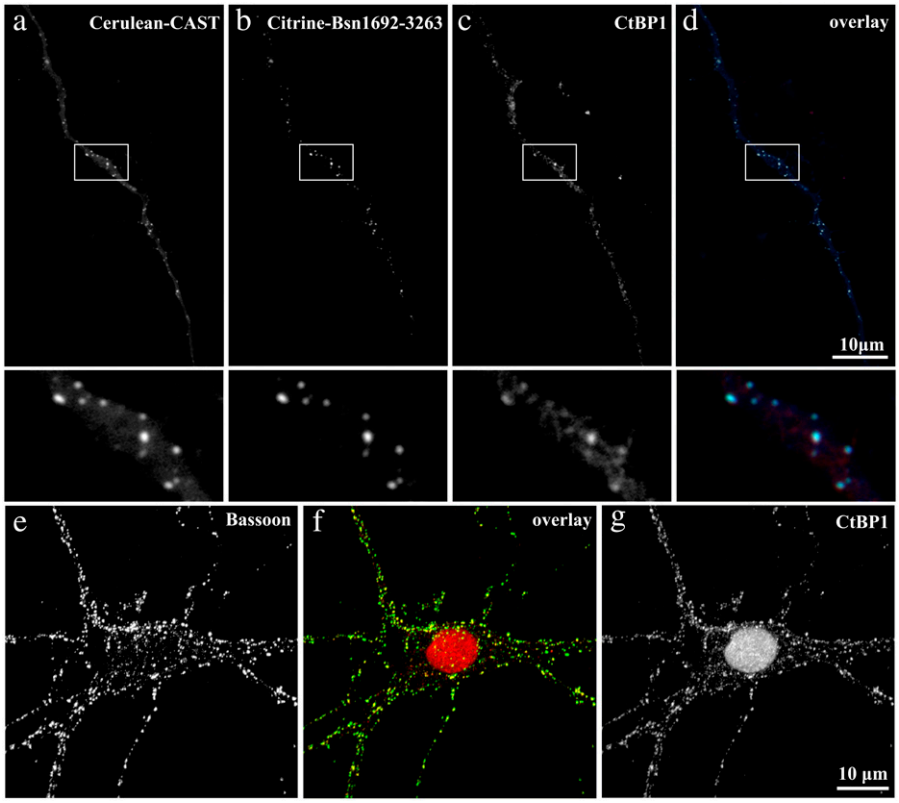

FIGURE 3 Colocalization of Bassoon, CtBP1, and CAST to the same intracellular complex in hippocampal neurons (*a–d*). Cells were transfected with Cerulean-CAST (*a*) and Citrine-Bsn1692-3263 (*b*) and immunostained with anti-CtBP1-Alexa 594 (*c*). The overlay of the trimeric complex is given in *d*, where Cerulean-CAST, Citrine-Bsn1692-3263, and CtBP1 are shown in green, red, and blue, respectively. (*e–g*) In the presence of Bassoon (*green*), CtBP1 (*red*) colocalized with Bassoon-containing complexes at DIV 16, most of which are likely to represent synapses.

high contamination from cell autofluorescence (~5- to 10-fold) at the excitation wavelength used, discrimination of energy transfer from cellular artifacts was difficult. Therefore, a brighter, shorter fragment of it, namely Bsn1692-3263 tagged with Cerulean, was used for the purpose (see Fig. 7). This construct showed a presynaptic recruitment similar to the full-length construct (16).

Bsn1692-3263 showed high aggregating properties when expressed in COS-7 cells. As a result, though the fluorescence emission spectrum was unaffected, the fluorescence decay of Cerulean Bsn1692-3263 was deviated, resulting in a third short lifetime component of 0.18 ± 0.05 ns (τ_3) (Table 1, Fig. 5, *a* and *b*). A cellular variability of this lifetime component was observed (with contributions <20%) due to the aggregating nature of Bsn1692-3263. DAS showed similar distributions for all three lifetimes with positive preexponential factors (Fig. 5 *c*). The contribution of the short lifetime component resulted in a reduction of the mean lifetime of this construct to 2.09 ± 0.17 ns at its emission peak (Table 1), which displayed no deviation along the wavelength axis similar to Cerulean alone (Fig. 5 *d*).

Coexpression of Cerulean-Bsn1692-3263 and Citrine-CtBP1 resulted in significant differences in the fluorescence emission spectra as well as the decay of both probes (Fig. 5, *a* and *b*). A Citrine enhancement at 529 nm in the spectra arose due to energy transfer (Fig. 5 *a*). The absolute values of different lifetimes of Cerulean-Bsn1692-3263 remained unchanged in the presence of FRET, though significant changes in the contributions of individual lifetimes were observed (Table 1). For the FRET sample, the contribution of τ_1 decreased from 44% to 24%, whereas contributions of τ_2 and τ_3 increased from 38% and 19% to 45% and 31%, respectively. This resulted in a reduction of the mean lifetime at the donor emission maxima from 2.09 ± 0.17 ns to 1.51 ± 0.10 ns (Table 1), which increased along the spectra to 2.87 ± 0.15 ns at the acceptor maxima (Fig. 5 *f*). DAS displayed negative preexponential factors for τ_2 and reduced contribution for τ_3 at the acceptor emission maxima (Fig. 5 *e*).

For a detailed analysis of the interaction, COS-7 cells expressing Cerulean-Bsn1692-3263 and Citrine-CtBP1 were imaged using the QA detector. Small ROIs were defined, and the corresponding fluorescence decays were analyzed for the donor and the acceptor probes simultaneously (Fig. 6, *a* and *b*). Multiexponential analysis revealed similar lifetimes as observed with the point detector (Table 2), and the quality of decay fits of both donor and acceptor probes were confirmed (Fig. 6 *c*). The acceptor fluorescence decay displayed negative preexponential factors (<10%) for the 1.4 ns (τ_2) component. The lifetime distributions of the puncta were mapped for a deeper understanding of the complex formation (Fig. 6 *d*). Significant reduction in the donor mean lifetimes with a simultaneous increase in the mean lifetimes of the acceptor were observed, as indicated by the transition from blue to red in the lifetime scale. Small deviations in the fluorescence lifetimes from the two detectors were expected due to the differential illumination methods used.

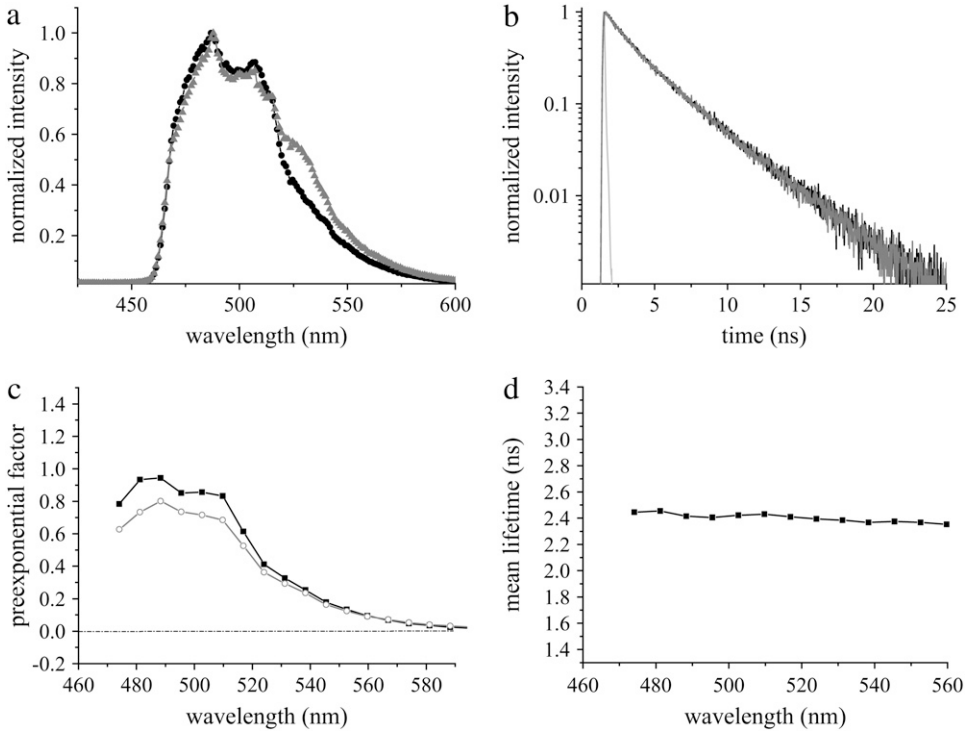

FIGURE 4 Fluorescence emission of Cerulean at 420 nm excitation in living COS-7 cells. (*a*) Comparison of fluorescence emission spectra of Cerulean alone (*black*) with coexpression of Cerulean and Citrine (*shading*). The fluorescence emission maximum for Cerulean was observed at 486 nm. A small Citrine component due to its high extinction coefficient was observed for the latter. (*b*) Fluorescence decay of Cerulean in the absence (*black*) and in the presence of Citrine (*shading*). IRF is shown in light shading. (*c*) DAS of Cerulean alone, which was unchanged in the presence of Citrine. Intensity decays were analyzed in 17 emission bands from 470 nm to 590 nm, and the preexponential factors of lifetimes τ_1 (*solid*) and τ_2 (*shading*) were plotted along the wavelength (Table 1). (*d*) Mean lifetimes of each emission band of Cerulean were plotted along the wavelength. Error bars are not shown due to their very small variability (<0.05 ns).

The FRET efficiencies were directly calculated from the differences in the donor mean lifetimes in the absence and presence of FRET. Using mean lifetimes of Cerulean-Bsn1692-3263 alone as τ_D (Table 1) and in the presence of Citrine-CtBP1 as τ_{DA} (Table 1), the FRET efficiency of the Bassoon-CtBP1 complex in COS-7 cells was 28%. The original energy transfer efficiency may be higher than this value due to the inclusion of the contribution of free conformers of donor not participating in FRET (6). But this influence of free donors on τ_{DA} could not be determined because of the aggregation of Bsn1692-3263 in COS-7 cells, which causes variability in control properties.

FLIM studies of Bassoon and CAST

Cerulean-Bsn1692-3263 and Citrine-CAST expressing COS-7 cells were imaged to study interactions between these proteins. The coexpressed cells revealed fluorescence dynamics (Table 1) similar to the donor control alone (i.e., Cerulean-Bsn1692-3263), except for a slight Citrine enhancement in the fluorescence emission spectra (Supplementary Material Fig. 5, *a* and *b*). A slight reduction in the mean lifetime of the coexpressed sample at the donor emission maxima was observed (1.93 ± 0.14 ns), which increased to 2.17 ± 0.24 ns at the acceptor emission maxima. Similar to the previous case,

TABLE 1 The decay kinetics of Cerulean and its fusion constructs in COS-7 cells in the absence and presence of FRET

Construct	*n*	τ_1%	τ_1 (ns)	τ_2%	τ_2 (ns)	τ_3%	τ_3 (ns)	τ_{mean} (ns)
Cerulean	5	56 ± 1	3.37 ± 0.03	45 ± 1	1.32 ± 0.05	-	-	2.46 ± 0.04
Cerulean+Citrine	5	57	3.32 ± 0.02	43	1.23 ± 0.06	-	-	2.41 ± 0.04
Cerulean-Bsn1692-3263	5	44 ± 5	3.35 ± 0.12	38 ± 2	1.56 ± 0.12	19 ± 5	0.23 ± 0.07	2.09 ± 0.17
Cerulean-Bsn1692-3263+Citrine-CtBP1	5	24 ± 2	3.39 ± 0.06	45 ± 2	1.42 ± 0.11	31 ± 2	0.20 ± 0.10	1.51 ± 0.10
Cerulean-Bsn1692-3263+Citrine-CAST	9	34 ± 6	3.41 ± 0.23	44 ± 4	1.60 ± 0.21	22 ± 4	0.31 ± 0.12	1.93 ± 0.14
Cerulean-CtBP1	7	58 ± 1	3.44 ± 0.04	42 ± 1	1.39 ± 0.08	-	-	2.57 ± 0.07
Cerulean-CtBP1 + Citrine-CAST	8	60 ± 1	3.41 ± 0.05	41 ± 1	1.29 ± 0.07	-	-	2.55 ± 0.07
Cerulean-CtBP1 + Citrine-CAST + *Bsn1692-3263	12	58 ± 2	3.24 ± 0.04	42 ± 2	1.06 ± 0.12			2.33 ± 0.11
Cerulean-Bsn1692-3263+Citrine-CtBP1+ Citrine-CAST	10	24 ± 1	3.37 ± 0.04	49 ± 3	1.39 ± 0.08	28 ± 2	0.24 ± 0.07	1.54 ± 0.07

The fluorescence lifetimes of Cerulean were not perturbed in the presence of coexpressed Citrine in the same cell. However, significant changes in the properties of Cerulean were observed depending on the protein to which it was tagged as well as in the presence of energy transfer. The donor mean lifetimes displayed significant reduction in the presence of FRET. The lifetimes are denoted τ_1, τ_2, and τ_3, and their corresponding contributions at the donor emission maxima are denoted τ_1%, τ_2%, and τ_3%. τ_{mean} represents the mean lifetime at the donor emission maxima. Errors <1% for the contributions are not shown. The number of independent measurements is denoted *n*. All data were recorded using the point detector. *Bsn1692-3263 refers to the untagged Bsn1692-3263.

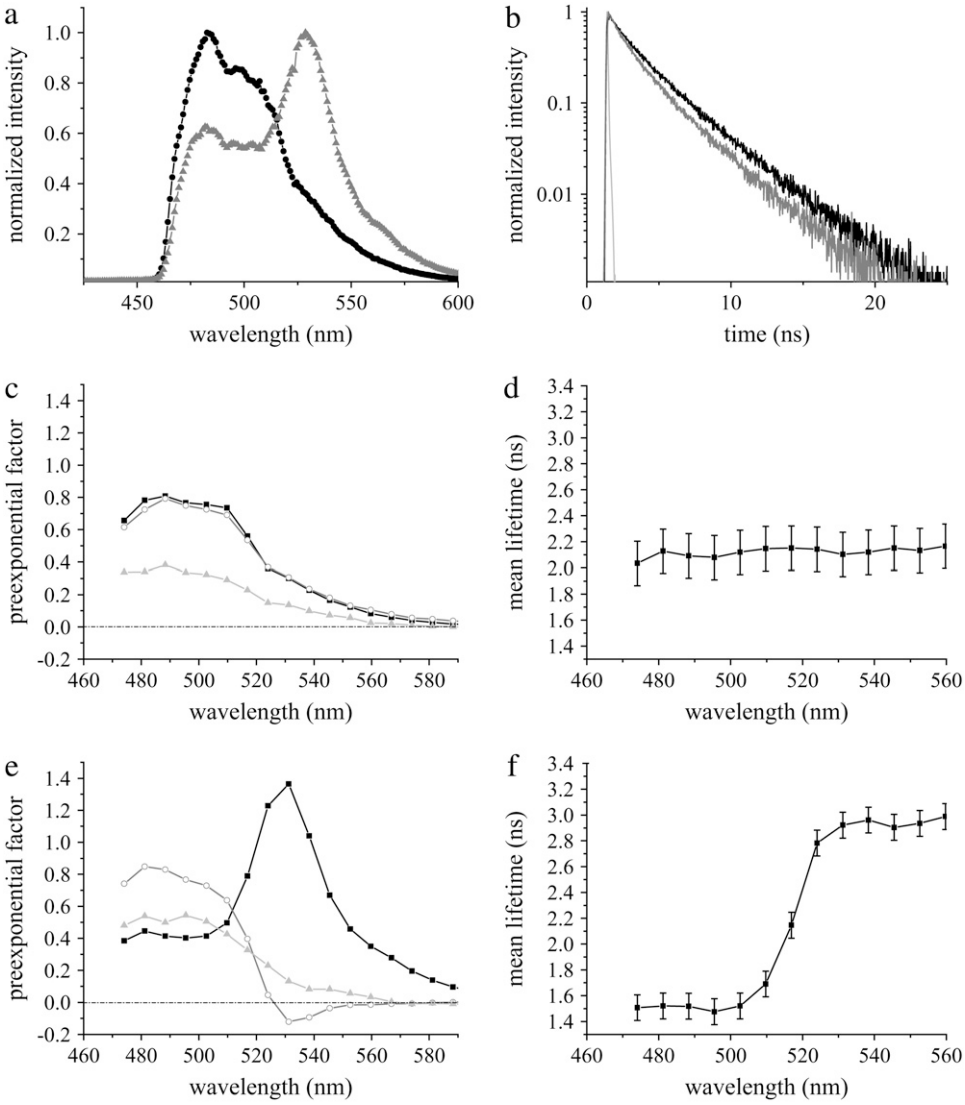

FIGURE 5 Fluorescence emission of Cerulean-Bsn1692-3263 in the absence and presence of Citrine-CtBP1 in living COS-7 cells. (*a*) Comparison of fluorescence emission spectra of Cerulean-Bsn1692-3263 (*black*) with the FRET sample (*shading*). A significant Citrine enhancement was observed in the presence of FRET. (*b*) Fluorescence decay of Cerulean-Bsn1692-3263 in the FRET sample (*shading*) was shorter compared to the control (*black*). IRF is shown in light shading. (*c*) DAS of control Cerulean-Bsn1692-3263. The preexponential factors of lifetimes τ_1 (*solid*), τ_2 (*shading*), and τ_3 (*light shading*) were plotted along the wavelength (Table 1). (*d*) Mean lifetimes of each emission band were plotted along the wavelength for Cerulean-Bsn1692-3263. The variability between the cells is represented by error bars, which shows deviation due to the aggregating nature of the construct. (*e*) DAS of the FRET sample, Cerulean-Bsn1692-3263+Citrine-CtBP1. The preexponential factors of lifetimes τ_1 (*solid*), τ_2 (*shading*), and τ_3 (*light shading*) (see Table 1) were plotted along the wavelength. Negative amplitudes were observed for τ_2 at the acceptor emission maximum in the presence of FRET. (*f*) Mean lifetimes of each emission band were plotted with error bars along the wavelength for the FRET sample.

energy transfer efficiencies were calculated from the donor mean lifetimes of the control and the coexpressed sample (Table 1). The results indicated a low energy transfer efficiency of 8%, which could be due to the large distance between the fluorophores of the interacting molecules. This was in accordance with the reduction of the contribution of τ_1 with a simultaneous increase in the contributions of the short lifetime components at the donor maxima of the coexpressed sample (Table 1), compared to the control. The large deviations in the lifetimes, particularly in τ_1 (Table 1), could be attributed to the highly oligomerizing nature of Bsn1692-3263 and CAST (26), which could also result in the lowering of acceptor mean lifetimes.

FLIM studies of CtBP1 and CAST

COS-7 cells expressing CtBP1 and CAST were measured to study interactions between the proteins in the absence of Bassoon. Cerulean-CtBP1 alone as well as the coexpressed sample of Cerulean-CtBP1 with Citrine-CAST showed fluorescence dynamics very similar to Cerulean (Table 1, Supplementary Material Fig. 5, *c* and *d*). The results indicated that there is no direct interaction between the two proteins in COS-7 cells, confirming the observation of Fig. 2, *e–g*, that coexpression of CAST does not change the endogenous localization of CtBP1.

Interaction studies of Bassoon, CtBP1, and CAST

To check whether Bassoon can simultaneously bind CtBP1 and CAST, the fluorescence dynamics of Cerulean-CtBP1 and Citrine-CAST were monitored in the presence of untagged Bsn1692-3263 (Supplementary Material Fig. 5, *e* and *f*) as well as the untagged full-length Bsn construct. For the triple-transfected cells, the mean lifetimes at the donor emission maxima showed a slight reduction, to 2.33 ± 0.11 ns (Table 1). The influence of the aggregating character of Bsn1692-3263 on Cerulean-CtBP1 dynamics was counter-

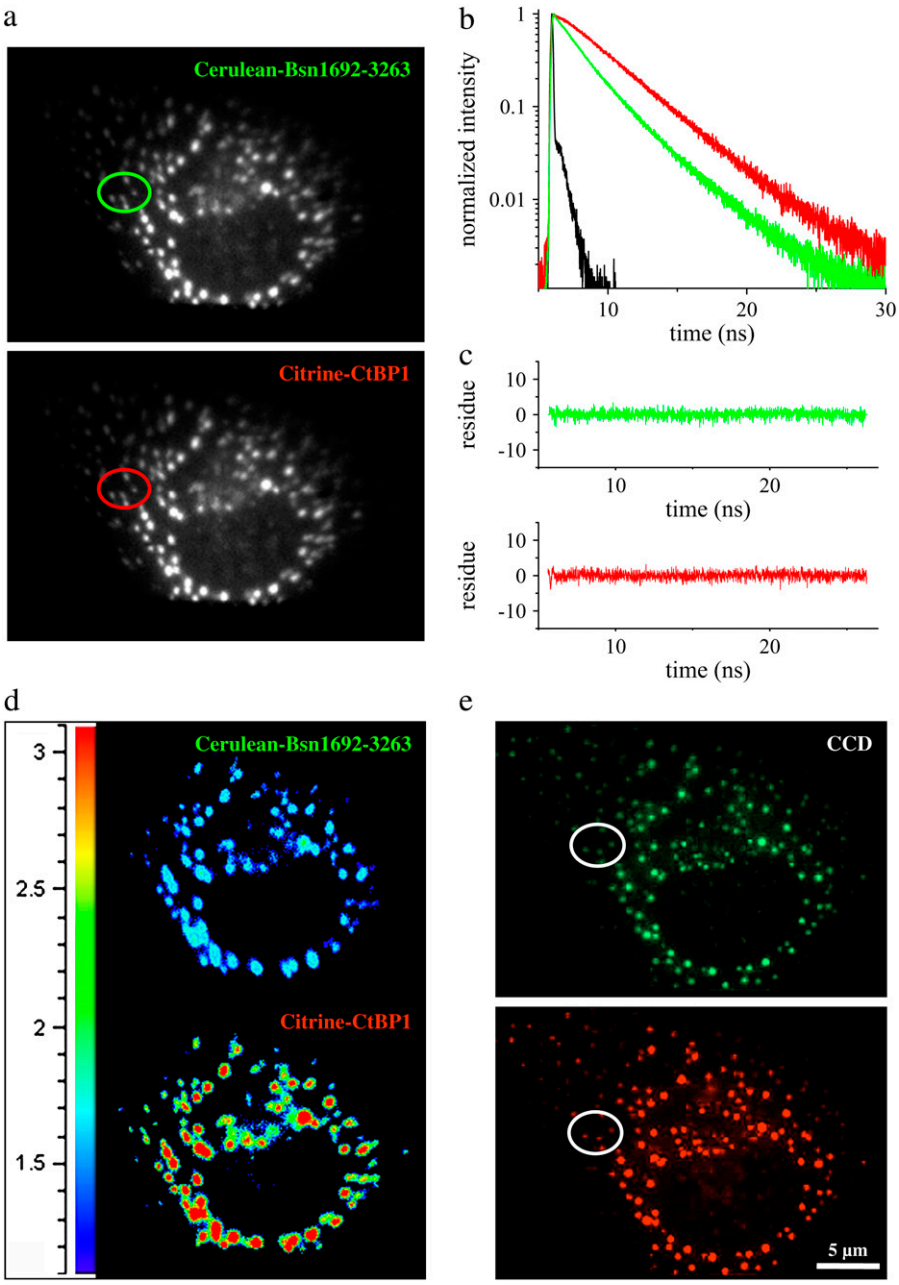

FIGURE 6 COS-7 cells coexpressing Cerulean-Bsn1692-3263 and Citrine-CtBP1 measured by the imaging detector. (*a*) The fluorescence emission was split into Cerulean-Bsn1692-3263 and Citrine-CtBP1 emission bands as shown. Selected ROIs are indicated by colored circles. (*b*) Fluorescence decays from corresponding ROIs marked in *a*. In the presence of energy transfer, Cerulean-Bsn1692-3263 (*green*) showed short fluorescence decay with a simultaneous rise for Citrine-CtBP1 (*red*). IRF is shown in black. (*c*) The quality of the individual fits (donor-*green*, acceptor-*red*) is shown by the distribution of the residues. (*d*) The lifetime distribution map of the FRET sample. The lifetimes increased significantly from the donor (*top*) to the acceptor (*bottom*), indicated by the transition from blue to red in the lifetime scale. (*e*) In the corresponding fluorescence images from the CCD camera, the green and red spots denote the donor and acceptor channels, respectively.

checked by coexpressing the proteins to exclude any differences in the donor properties. Donor mean lifetimes in this case were very similar ($\tau_D = 2.51 \pm 0.04$ ns) to that of Cerulean-CtBP1 alone. From the donor mean lifetimes of the control (τ_D) and of the coexpressed sample (τ_{DA}, Table 1), the results indicated a very low energy transfer efficiency, 7%, pointing to a simultaneous binding of CtBP1 and CAST to Bassoon.

A different strategy was adopted to confirm this hypothesis. COS-7 cells expressing Cerulean-Bsn1692-3263 together with Citrine-CtBP1 and Citrine-CAST were measured. FLIM measurements between Bsn1692-3263 and CAST have shown a reduced FRET efficiency, with donor mean lifetimes close to that of the control (Table 1). Therefore, if the binding of CtBP1 and CAST on Bassoon were competitive, or if different Bassoon molecules were binding to CtBP1 and CAST, an overall decrease in the FRET efficiency between Bassoon and CtBP1 would be expected in the presence of coexpressed CAST. This should result in an increase in the donor mean lifetime of the triple-coexpressed sample close to the control, in contrast to the FRET pair Bassoon-CtBP1. Interestingly, the fluorescence kinetics (Table 1) and the resulting FRET efficiency between the Bassoon-CtBP1 pair remained unchanged ($E = 26\%$) in the presence of Citrine-CAST. The presence of all three proteins in the same complexes was ensured by immunofluorescence stainings of the measured cells with antibodies against CtBP1 and CAST. The results

TABLE 2 Fluorescence dynamics of Cerulean in COS-7 cells measured by the imaging detector in the absence and presence of FRET

Construct	τ_1%	τ_1 (ns)	τ_2%	τ_2 (ns)	τ_3%	τ_3 (ns)	τ_{mean} (ns)
Cerulean-Bsn1692-3263	40 ± 3	3.14 ± 0.09	41 ± 2	1.57 ± 0.07	19 ± 3	0.39 ± 0.12	1.98 ± 0.11
Cerulean-Bsn1692-3263 + Citrine-CtBP1	21 ± 3	3.3 ± 0.23	48 ± 4	1.44 ± 0.20	31 ± 5	0.38 ± 0.12	1.49 ± 0.18

The fluorescence lifetimes of Cerulean-Bsn1692-3263 as well as their fractional contributions were significantly changed in the presence of FRET, which resulted in a drastic decrease of donor mean lifetimes. The lifetimes are denoted τ_1, τ_2, and τ_3, and their corresponding contributions are denoted τ_1%, τ_2%, and τ_3% in the donor emission band. τ_{mean} represents the mean lifetime in the donor channel. The values shown are from five independent measurements by the imaging detector, with at least six ROIs selected from each cell.

indicated that there was no inhibition for the Bassoon-CtBP1 interaction in the presence of CAST, thus confirming the model of simultaneous binding of CtBP1 and CAST on the same Bassoon molecule. The different binding studies and the resulting FRET efficiencies are summarized in Fig. 7.

Interaction studies of Bassoon and CtBP1 by FRET-FLIM in living hippocampal neurons

Since the maximum FRET efficiency was observed between Bassoon and CtBP1, this interaction was further studied at synaptic complexes of hippocampal neurons. To overrule any deviations in the photophysical properties of Cerulean due to ionic variations in neurons along development (6), neurons expressing the donor fusion construct Cerulean-Bsn1692-3263 were imaged at young (DIV 9) as well as at mature (DIV 16) stages. Data presented here are from mature cells (DIV 16). Irrespective of the maturation stage of neurons, the fluorescence dynamics of Cerulean-Bsn1692-3263 remained unchanged, with the emission maximum at 486 nm (Fig. 8 *a*). In contrast to the triexponential decay of this construct in COS-7 cells, a biexponential fluorescence decay was observed in neurons. The multiexponential analysis revealed lifetimes of 3.14 ± 0.14 ns (τ_1) and 1.29 ± 0.16 ns (τ_2) with contributions of 60% ± 3% and 40% ± 3%, respectively, at its emission maxima (Table 3, Fig. 8 *b*). This resulted in a mean lifetime of 2.39 ± 0.15 ns at its emission maxima, which remained constant over the spectra (Fig. 8 *d*). DAS displayed positive values for the preexponential factors of all lifetimes (Fig. 8 *c*). The unchanging fluorescence dynamics of Cerulean-Bsn1692-3263 at different stages of neuronal development (DIV 9 and 16) confirmed the photostability of the probe, proving it to be a suitable FRET donor in living neurons. The biexponential fluorescence decay of recombinant Bassoon in neurons indicated the lower aggregation probability of the construct when expressed in its natural environment (17).

Fluorescence emission from processes of mature neurons at DIV 16 expressing Cerulean-Bsn1692-3263 and Citrine-CtBP1 was collected to study the interactions at synapses. The area of illumination was restricted by closing an iris in the beam path (see Materials and Methods). The fluorescence spectra collected from colocalizing complexes showed the donor emission maximum at 486 nm with an additional Citrine enhancement at 529 nm (Fig. 8 *a*), the latter arising due to energy transfer. The fluorescence decays at the donor maxima were fit with lifetimes of 3.29 ± 0.04 ns (τ_1; 25%), 1.29 ± 0.11 ns (τ_2; 44%), and 0.16 ± 0.04 ns (τ_3; 31%) (Table 3, Fig. 8 *b*), resulting in a mean lifetime of 1.44 ± 0.16 ns. Due to energy transfer, the mean lifetime increased to 2.89 ± 0.14 ns (Fig. 8 *f*) at the acceptor emission peak; the increase was accompanied by a dramatic change in the contributions of τ_1 (84% ± 6%), τ_2 (10% ± 4%), and τ_3 (<10%), with τ_2 displaying negative preexponential factors at the same (Fig. 8 *e*).

Subsequent to the spectroscopic analysis with the point detector, subcellular compartments of the same neuronal processes were measured using the imaging detector (Fig. 9). The deduced lifetimes from the multiexponential analysis showed minor changes from the point detector. Cerulean-Bsn1692-3263 in the colocalized complexes displayed faster fluorescence decay compared to the donor control (Fig. 9 *b*). This was accompanied by a rise in the acceptor decay kinetics. The lifetime distribution map also indicated the presence of energy transfer in the synaptic complexes, with reduced mean lifetimes for Cerulean-Bsn1692-3263 increasing significantly in the acceptor channels (Fig. 9 *c*). This was confirmed from the multiexponential analysis, which revealed negative contributions (<1%) for τ_2 in the acceptor channels. The difficulty (due to its lower wavelength resolution) in observing negative preexponential factors using the imaging detector instead of the point detector has been discussed (6). The imaged cells were fixed and immunostained with antibodies against the postsynaptic marker SAP90/PSD-95; this identified many of the colocalized complexes of Bassoon and CtBP1 specifically as synapses (Fig. 9 *d*).

FRET efficiency calculations were performed in the same way as those for COS-7 cells. For interactions in the processes, using τ_D of Cerulean-Bsn1692-3263 (Table 3) and τ_{DA} of the FRET sample (Table 3), the FRET efficiency was calculated to be 40% in synapses. Similar FRET efficiencies were also observed for Bassoon-CtBP1 complexes in the soma. The difference in efficiency between neurons and COS-7 cells may be attributed to the variation in the donor properties due to the differential aggregation of Bassoon between the cell types.

DISCUSSION

Using a novel FLIM approach with simultaneous acquisition of donor and acceptor decays and DAS to verify FRET, we confirmed a direct physical association of synaptic proteins

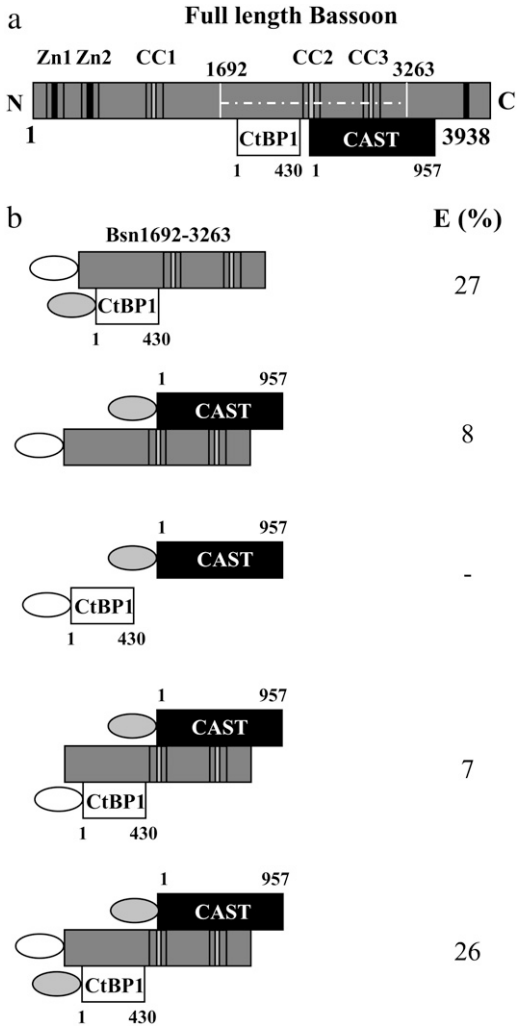

FIGURE 7 Combinatorial expressions of Bassoon, CAST, and CtBP1 in COS-7 cells. (*a*) Scheme illustrating the proposed binding regions for CtBP1 and CAST on Bassoon (11,14). The white lines indicate the projection of Bsn1692-3263 on the full-length construct. Zn denotes the zinc fingers and CC the coiled coil domains. (*b*) The different binding studies for determining the association of the molecules involved in the trimeric complex. The maximum FRET efficiency (*E*) was observed between Bassoon and CtBP1, which remained unchanged in the presence of CAST. Bassoon was essential for the formation of a trimeric complex of these proteins, without which no association between CtBP1 and CAST was observed. The data confirmed the simultaneous association of CtBP1 and CAST with the same Bassoon molecule. The white and shaded ellipses represent Cerulean and Citrine, respectively.

Bassoon and CtBP1 in living COS-7 cells as well as in living neurons. Despite deviations in the photophysical properties of fluorophores depending on the protein component to which they were fused, interactions were associated with significant changes in the donor and acceptor mean lifetimes as well as negative amplitudes for the FRET lifetimes at the acceptor emission maxima. Bassoon was observed to be essential for forming a macromolecular complex with CtBP1 and CAST. The data provided a direct confirmation of the interaction of Bassoon and CtBP1 at synapses of living hippocampal neurons.

Though Bassoon, CtBP1, and CAST were recruited to the same molecular complexes (Figs. 2 and 3), it was essential to understand whether CtBP1 and CAST could bind simultaneously to Bassoon or whether the binding of the proteins would be competitive. The capability of Bassoon to simultaneously bind the two interaction partners was confirmed from FLIM studies.

Cerulean-Bsn1692-3263, when expressed in COS-7 cells, exhibited complex behavior and had a shorter lifetime component in the fluorescence decay (Table 1, Fig. 5 *b*). This was in agreement with previous reports that showed the tendency of the protein to form clusters in nonneuronal cells (16). Fluorescence characterization of the different deletion constructs of Bassoon traced this property of aggregation to the second coiled-coil domain of the protein, when overexpressed. The comparison of the fluorescence dynamics of Cerulean alone with its fusion constructs showed how the properties of a fluorescent probe depend on the protein component to which it is fused (Table 1). The higher aggregation tendency as well as the largeness of the fused protein may affect the intrinsic properties of fluorophores. This may result in a variation in the photophysical properties of fluorophores of recombinant proteins from those of the control. This was also in accordance with the biexponential fluorescence decay of the same construct (Cerulean- Bsn1692-3263) in neurons, where lower aggregation was observed (Fig. 8 *c*).

In the presence of Citrine-CtBP1, Cerulean-Bsn1692-3263 showed FRET with DAS displaying negative preexponential factors for τ_2, indicating the involvement of this lifetime in energy transfer (Figs. 5 *e* and 8 *e*). The change in sign at the acceptor emission maxima evolved only due to the presence of energy transfer (25). The comparison of contributions of individual lifetimes further affirmed the suitability of the approach used here, whereby FRET could be distinguished even in the presence of additional lifetime components from the donor, as in COS-7 cells (Table 1). Rigorous error analysis performed on multiple lifetimes confirmed the reliability of the deviations in fluorescence properties in the presence of energy transfer.

For a detailed analysis of the Bassoon-CtBP1 interaction at individual puncta, recordings were done using the imaging detector. Small ROIs corresponding to groups of these complexes (Figs. 6 and 9) were selected for multiexponential analysis. The morphological distribution of mean lifetimes was obtained from the FLIM map (Figs. 6 *d* and 9 *c*). These combined approaches, in turn, gave more extensive information on the heterogeneity of protein interactions inside a cell at normal conditions and confirmed the presence of energy transfer.

There was no direct way to determine whether CtBP1 and CAST can be recruited to the same Bassoon molecule, since the coexpression of these proteins with the untagged Bassoon

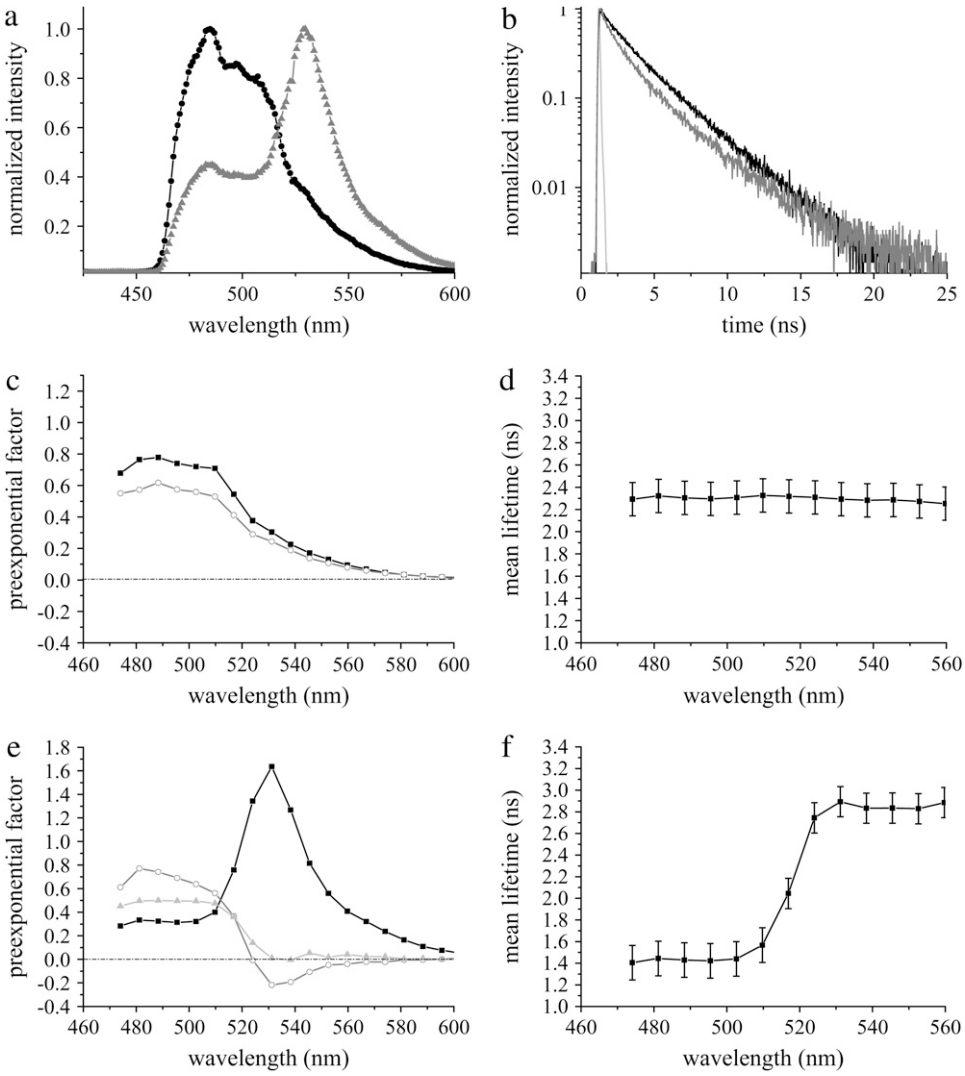

FIGURE 8 Fluorescence emission dynamics of Cerulean-Bsn1692-3263 in the absence ($n = 8$) and presence ($n = 5$) of Citrine-CtBP1 at synapses of living neurons at DIV 16. (*a*) Comparison of fluorescence emission spectra of Cerulean-Bsn1692-3263 (*black*) with the FRET sample (*shading*). A significant Citrine enhancement was observed in the presence of FRET. (*b*) Fluorescence decay of Cerulean-Bsn1692-3263 in the FRET sample (*shading*) was shorter than the control (*black*). IRF is shown in light shading. (*c*) DAS of Cerulean-Bsn1692-3263 in living neurons. The preexponential factors of lifetimes τ_1 (*solid*) and τ_2 (*shading*) (see Table 3) were plotted along the wavelength. The preexponential factors showed only positive values. (*d*) Mean lifetimes of each emission band of Cerulean-Bsn1692-3263 was plotted along the wavelength. No deviations along the spectra were observed. (*e*) DAS of the FRET sample, Cerulean-Bsn1692-3263+Citrine-CtBP1. The preexponential factors of lifetimes τ_1 (*solid*), τ_2 (*shading*), and τ_3 (*light shading*) (Table 3) were plotted along the wavelength. Negative amplitudes were observed for τ_2 at the acceptor emission maximum in the presence of FRET. (*f*) The plot of mean lifetimes showed significant deviations along the wavelength in the presence of FRET.

did not result in a strong energy transfer. Therefore, an alternative strategy for confirming this model was applied in which all three proteins with fluorescent tags were coexpressed. The results indicated no difference from the coexpression of Bassoon and CtBP1, thus confirming that the proposed trimeric complex can be formed. The different binding strategies proved Bassoon to be an essential linker in the formation of such multiprotein complexes linking CtBP1 and CAST and potentially other molecules of the CAZ network inside a cell.

The CAZ proteins known to date, including CAST, RIM1, Munc13-1, Bassoon, and Piccolo, have been proposed to form a large dynamic multimolecular complex in vivo (12). Here, a direct physical interaction between Bassoon and CtBP1 was shown in synaptic complexes of living hippocampal neurons (Figs. 8 and 9). Although the physiological

TABLE 3 Fluorescence dynamics of Cerulean in living hippocampal neurons in the absence and presence of FRET

Construct	n	τ_1%	τ_1 (ns)	τ_2%	τ_2 (ns)	τ_3%	τ_3 (ns)	τ_{mean} (ns)
Cerulean-Bsn1692-3263	8	60 ± 3	3.14 ± 0.14	44 ± 3	1.29 ± 0.16	-	-	2.39 ± 0.15
Cerulean-Bsn1692-3263+Citrine-CtBP1	5	25 ± 6	3.29 ± 0.04	44 ± 5	1.29 ± 0.11	31 ± 3	0.16 ± 0.04	1.44 ± 0.16

Similar to the results observed in COS-7 cells, the contributions of the lifetimes of Cerulean-Bsn1692-3263 was significantly affected in the presence of Citrine-CtBP1. The lifetimes are denoted τ_1, τ_2, and τ_3, and their corresponding contributions at the donor emission maxima are denoted τ_1%, τ_2%, and τ_3%. τ_{mean} is the mean lifetime at the donor emission maxima. The number of independent measurements is denoted n. The data were taken from the synaptic complexes in axonal processes of hippocampal neurons, using the point detector.

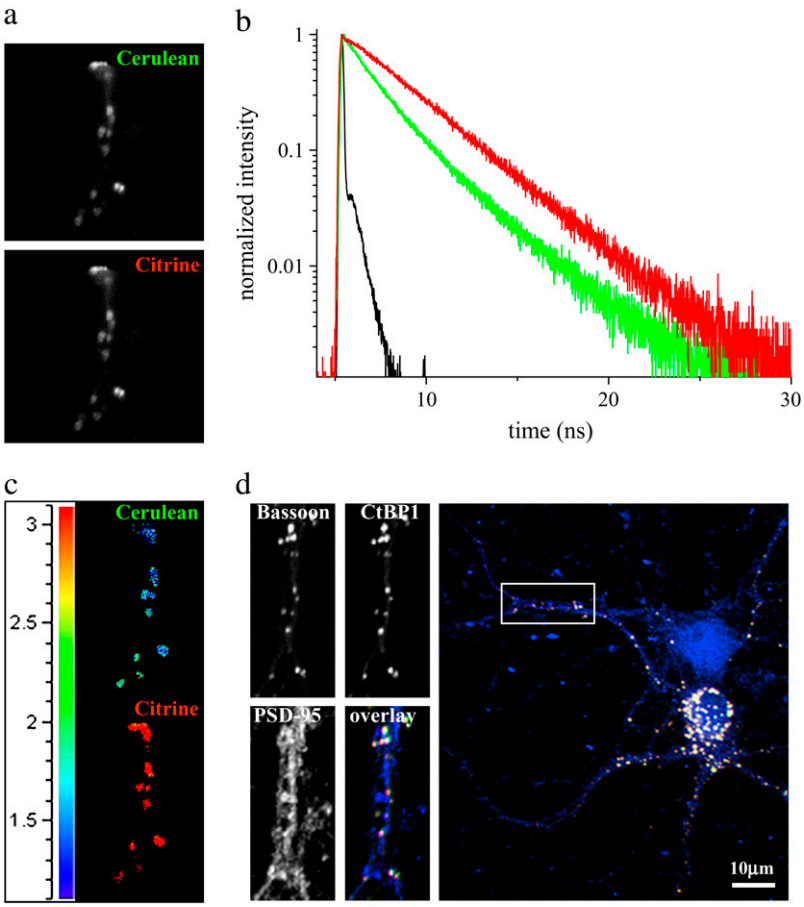

FIGURE 9 Processes of hippocampal neurons at DIV 16 coexpressing Cerulean-Bsn1692-3263 and Citrine-CtBP1, as measured by the imaging detector. (*a*) The fluorescence emission was split into Cerulean-Bsn1692-3263 and Citrine-CtBP1 emission bands as shown. (*b*) In the presence of energy transfer, Cerulean-Bsn1692-3263 (*green*) showed a short fluorescence decay with a simultaneous rise for Citrine-CtBP1 (*red*) with negative amplitudes for τ_2. IRF is shown in black. (*c*) The lifetime distribution map of the FRET sample. The lifetimes increased significantly from the donor (*top*) to the acceptor (*bottom*), indicated by the transition from blue to red in the lifetime scale. (*d*) The imaged cells were fixed and immunostained with antibodies against the postsynaptic marker protein Sap90/PSD-95, which identified the colocalized complexes of Bassoon and CtBP1 to be presynapses. Confocal images were obtained from similar regions as measured by FLIM. In the overlay image, Cerulean-Bsn1692-3263, Citrine-CtBP1, and PSD-95 are shown in green, red, and blue, respectively.

significance of this interaction is not yet known, the interaction of Bassoon and CAST has been shown to be implicated in synaptic transmission (11,27). The interaction of these proteins could play a role in the molecular arrangement of the CAZ. Due to its capacity to form oligomers (26), CAST could serve as a cross-linker of other CAZ molecules, including Bassoon and its sister molecule Piccolo. CtBP1 is a multifunctional protein involved in the fission of vesicles from the trans-Golgi network (28). It was originally identified as a transcription corepressor localized in the nucleus (15). Moreover, the paralog CtBP2 is part of a larger molecule called Ribeye, which is a major structural component of synaptic ribbons—a specialization of the CAZ at ribbon synapses in retinal photoreceptors or inner ear hair cells (29,30). Data presented here suggest recruitment of CtBP1 to the CAZ network via its association with Bassoon.

CONCLUSIONS

The nanoscale organization of the CAZ is thought to be vital for the efficient functioning of presynapses. The potential for the formation of a trimeric complex with the simultaneous binding of CtBP1 and CAST on the same Bassoon molecule was proven by FRET using time domain FLIM. The formation of such networks of proteins could be the basic mechanism by which Bassoon serves its scaffolding role in the molecular organization of the CAZ. The studies were extended to confirm direct physical association of Bassoon and CtBP1 in synaptic complexes of living hippocampal neurons. The association and dissociation of such presynaptic complexes could, in turn, affect the synapse formation, maintenance, and plasticity. Further studies are necessary to better understand the molecular mechanisms that spatially and temporally regulate the coupling of the CAZ protein complex and the neurotransmitter release machinery. Though FRET-FLIM studies in living neurons were highly challenging due to the different cellular influences involved, time-resolved imaging under optimal conditions with proper characterization resulted in a wealth of information regarding synaptic scaffolding mechanisms that, to our knowledge, are not available by any other existing method.

SUPPLEMENTARY MATERIAL

To view all of the supplemental files associated with this article, visit www.biophysj.org.

The authors thank Prof. D. W. Piston, Vanderbilt University, Tennessee, and Prof. R. Y. Tsien, University of California, San Diego, for kindly

providing the p-Cerulean and p-Citrine cDNAs, respectively. We are grateful to Kathrin Gruss for her expert technical assistance.

This work was supported by the Deutsche Forschungsgemeinschaft (ZU59/5-1/2 and FOR 521-HA3498/1) to W.Z. and (AL 1115/1-1) to W.D.A.; the European Commission NMP4-CT-2005-013880 and MRTN-CT-2005-0198481 to W.Z. and SynScaff to E.D.G.; as well as the Land Saxony Anhalt (N2), the Fonds der Chemischen Industrie and Max Planck Award of the Humboldt Foundation and the Max Planck Society to E.D.G.

REFERENCES

1. Ballestrem, C., and B. Geiger. 2005. Application of microscope-based FRET to study molecular interactions in focal adhesions of live cells. *Methods Mol. Biol.* 294:321–334.
2. Jares-Erijman, E. A., and T. M. Jovin. 2003. FRET imaging. *Nat. Biotechnol.* 21:1387–1395.
3. Chen, Y., J. D. Mills, and A. Periasamy. 2003. Protein localization in living cells and tissues using FRET and FLIM. *Differentiation.* 71:528–541.
4. van Munster, E. B., and T. W. Gadella. 2005. Fluorescence lifetime imaging microscopy (FLIM). *Adv. Biochem. Eng. Biotechnol.* 95:143–175.
5. Nair, D. K., M. Jose, T. Kuner, W. Zuschratter, and R. Hartig. 2006. FRET-FLIM at nanometer spectral resolution from living cells. *Opt. Express.* 14:12217–12229.
6. Jose, M., D. K. Nair, C. Reissner, R. Hartig, and W. Zuschratter. 2007. Photophysics of Clomeleon by FLIM: discriminating excited state reactions along neuronal development. *Biophys. J.* 92:2237–2254.
7. Dresbach, T., B. Qualmann, M. M. Kessels, C. C. Garner, and E. D. Gundelfinger. 2001. The presynaptic cytomatrix of brain synapses. *Cell. Mol. Life Sci.* 58:94–116.
8. Gundelfinger, E. D., M. M. Kessels, and B. Qualmann. 2003. Temporal and spatial coordination of exocytosis and endocytosis. *Nat. Rev. Mol. Cell Biol.* 4:127–139.
9. tom Dieck, S., L. Sanmarti-Vila, K. Langnaese, K. Richter, S. Kindler, A. Soyke, H. Wex, K. H. Smalla, U. Kampf, J. T. Franzer, M. Stumm, C. C. Garner, and E. D. Gundelfinger. 1998. Bassoon, a novel zinc-finger CAG/glutamine-repeat protein selectively localized at the active zone of presynaptic nerve terminals. *J. Cell Biol.* 142:499–509.
10. Fenster, S. D., W. J. Chung, R. Zhai, C. Cases-Langhoff, B. Voss, A. M. Garner, U. Kaempf, S. Kindler, E. D. Gundelfinger, and C. C. Garner. 2000. Piccolo, a presynaptic zinc finger protein structurally related to bassoon. *Neuron.* 25:203–214.
11. Takao-Rikitsu, E., S. Mochida, E. Inoue, M. Deguchi-Tawarada, M. Inoue, T. Ohtsuka, and Y. Takai. 2004. Physical and functional interaction of the active zone proteins, CAST, RIM1, and Bassoon, in neurotransmitter release. *J. Cell Biol.* 164:301–311.
12. Schoch, S., and E. D. Gundelfinger. 2006. Molecular organization of the presynaptic active zone. *Cell Tissue Res.* 326:379–391.
13. Wang, Y., X. Liu, T. Biederer, and T. C. Sudhof. 2002. A family of RIM-binding proteins regulated by alternative splicing: implications for the genesis of synaptic active zones. *Proc. Natl. Acad. Sci. USA.* 99:14464–14469.
14. tom Dieck, S., W. D. Altrock, M. M. Kessels, B. Qualmann, H. Regus, D. Brauner, A. Fejtova, O. Bracko, E. D. Gundelfinger, and J. H. Brandstatter. 2005. Molecular dissection of the photoreceptor ribbon synapse: physical interaction of Bassoon and RIBEYE is essential for the assembly of the ribbon complex. *J. Cell Biol.* 168:825–836.
15. Corda, D., A. Colanzi, and A. Luini. 2006. The multiple activities of CtBP/BARS proteins: the Golgi view. *Trends Cell Biol.* 16:167–173.
16. Dresbach, T., A. Hempelmann, C. Spilker, S. tom Dieck, W. D. Altrock, W. Zuschratter, C. C. Garner, and E. D. Gundelfinger. 2003. Functional regions of the presynaptic cytomatrix protein bassoon: significance for synaptic targeting and cytomatrix anchoring. *Mol. Cell. Neurosci.* 23:279–291.
17. Dresbach, T., V. Torres, N. Wittenmayer, W. D. Altrock, P. Zamorano, W. Zuschratter, R. Nawrotzki, N. E. Ziv, C. C. Garner, and E. D. Gundelfinger. 2006. Assembly of active zone precursor vesicles: obligatory trafficking of presynaptic cytomatrix proteins Bassoon and Piccolo via a trans-Golgi compartment. *J. Biol. Chem.* 281:6038–6047.
18. Kuner, T., and G. J. Augustine. 2000. A genetically encoded ratiometric indicator for chloride: capturing chloride transients in cultured hippocampal neurons. *Neuron.* 27:447–459.
19. Rizzo, M. A., G. H. Springer, B. Granada, and D. W. Piston. 2004. An improved cyan fluorescent protein variant useful for FRET. *Nat. Biotechnol.* 22:445–449.
20. Griesbeck, O., G. S. Baird, R. E. Campbell, D. A. Zacharias, and R. Y. Tsien. 2001. Reducing the environmental sensitivity of yellow fluorescent protein. Mechanism and applications. *J. Biol. Chem.* 276:29188–29194.
21. Lippincott-Schwartz, J., and G. H. Patterson. 2003. Development and use of fluorescent protein markers in living cells. *Science.* 300:87–90.
22. Kemnitz, K., L. Pfeifer, R. Paul, and M. Coppey-Moisan. 1997. Novel detectors for fluorescence lifetime imaging on the picosecond time scale. *J Fluoresc.* 7:93–98.
23. Kapusta, P., R. Erdmann, U. Ortmann, and M. Wahl. 2003. Time-resolved fluorescence anisotropy measurements made simple. *J Fluoresc.* 13:179–183.
24. Beechem, J. M., and E. Haas. 1989. Simultaneous determination of intramolecular distance distributions and conformational dynamics by global analysis of energy transfer measurements. *Biophys. J.* 55:1225–1236.
25. Lakowicz, J. R. 1999. Principles of Fluorescence Spectroscopy. Kluwer Academic/Plenum Publishers, New York.
26. Deguchi-Tawarada, M., E. Inoue, E. Takao-Rikitsu, M. Inoue, T. Ohtsuka, and Y. Takai. 2004. CAST2: identification and characterization of a protein structurally related to the presynaptic cytomatrix protein CAST. *Genes Cells.* 9:15–23.
27. Altrock, W. D., S. tom Dieck, M. Sokolov, A. C. Meyer, A. Sigler, C. Brakebusch, R. Fassler, K. Richter, T. M. Boeckers, H. Potschka, C. Brandt, W. Loscher, D. Grimberg, T. Dresbach, A. Hempelmann, H. Hassan, D. Balschun, J. U. Frey, J. H. Brandstatter, C. C. Garner, C. Rosenmund, and E. D. Gundelfinger. 2003. Functional inactivation of a fraction of excitatory synapses in mice deficient for the active zone protein bassoon. *Neuron.* 37:787–800.
28. Nardini, M., S. Spano, C. Cericola, A. Pesce, A. Massaro, E. Millo, A. Luini, D. Corda, and M. Bolognesi. 2003. CtBP/BARS: a dual-function protein involved in transcription co-repression and Golgi membrane fission. *EMBO J.* 22:3122–3130.
29. Schmitz, F., A. Konigstorfer, and T. C. Sudhof. 2000. RIBEYE, a component of synaptic ribbons: a protein's journey through evolution provides insight into synaptic ribbon function. *Neuron.* 28:857–872.
30. Khimich, D., R. Nouvian, R. Pujol, S. Tom Dieck, A. Egner, E. D. Gundelfinger, and T. Moser. 2005. Hair cell synaptic ribbons are essential for synchronous auditory signalling. *Nature.* 434:889–894.